MATERIALE PLASTICE
https://revmaterialeplastice.ro
https://doi.org/10.37358/Mat.Plast.1964

Impact Behavior Analysis of 3-D Printed Honeycomb Structures

CONSTANTIN - ROMICA STOICA*, RALUCA MAIER, ANCA - MIHAELA ISTRATE, SEBASTIAN - GABRIEL BUCACIUC, ALEXANDRA DESPA
Romanian Research and Development Institute for Gas Turbine COMOTI, 220D Iuliu Maniu Av., 061126, Bucharest, Romania

Abstract: *The purpose of this paper is to evaluate the behaviour of 3D printed honeycomb structures under low velocity impact loading for their use in energy absorption applications. Additive manufacturing technologies are part of a growing field that represents high interest for industries such as aerospace, automotive and naval. This paper aims to determine the mechanical properties of a 3D printed polymer - Polylactic Acid (PLA) manufactured by FDM (Fused Deposition Modelling) technology. In this regard, first the material is characterized by low velocity impact dynamic experimental tests. A finite Element Analysis (FEA) is performed in LS-Dyna software in order to validate the results. The samples were manufactured by varying the infill percent to investigate the influence of different parameters on a batch of samples for every configuration. The 3D CAD modelling for impact tests samples were performed in Catia V5. Among wide range of cellular structures, honeycomb non-auxetic hexagonal cell pattern was selected in this study, assuring high strength/weight ratio. The amount of energy absorbed during the impact, the failure and degradation of the impacted specimens were monitored, following the analysis of experimental and numerical data. A fair agreement was obtained between experimental and numerical results, showing that honeycomb developed lightweight structures exhibits a proper energy absorption capacity, with a mechanism of release similar to metal or composite materials honeycombs.*

Keywords*: 3-D printing, cellular structures, FEM, low velocity impact*

1. Introduction

Driven by the increasingly stringent engineering application requirements to achieve engineering structures answering to requirements for both lightweight structures and energy absorption applications, particularly sandwich structures were developed in the last decade. Low-velocity impact protection has a particular interest in engineering applications. It induces more localized damage than quasi-static compression and less localized damage than high-velocity impact loading [1]. The deformation mechanism under high and low-velocity impact conditions is likely to be governed by localized material damage rather than global buckling.

Lightweight sandwich panels are nowadays extensively used in aerospace, marine, automotive, windmills and construction industries due to their high flexural stiffness-to-weight ratio, excellent thermal insulation and high energy absorption capability [2]. Sandwich panels consist of two thin but stiff face-sheets at the top and bottom of the panel separated by a lightweight and relatively thick core. The lightweight core connects the face-sheets with small increase in weight but provides sandwich panels with a high bending stiffness and buckling resistance [3] as well as an excellent shear stiffness and energy absorption capability [4].

Furthermore, emerging additive manufacturing technologies raised researchers and engineering interest in the last years due to its undisputable advantages in terms of performances and lower production costs. In recent years, 3-D printing experts have laid emphasis on designing and printing the cellular structures, since the key advantages (high strength to weight ratio, thermal and acoustical insulation properties) offered by these structures makes them highly versatile to be used in aerospace and automotive industries [5]. Fused deposition modelling (FDM) is an advanced additive manufacturing technology for creating structures based on thermoplastic materials.

**email:romica.stoica@comoti.ro*

This technique resorts to a spool of thermoplastic filament to be melted and extruded through a heated nozzle and, subsequently, deposited in two-dimensional layers that will form a 3D printed object [6,7]. Several studies have recently investigated 3D printing of poly-lactic acid (PLA) with biomass resources like cellulose, hemicellulose, lignin and whole biomass. Such biodegradable composites are better for the environment and can be used to replace non-biodegradable composites in a variety of applications [7]. Poly-lactic acid is characterized by good mechanical strength, but unfortunately, stiffness and the fragile nature of the breakage, drastically limits its usage. A wide range of applications are being conducted for improving flexibility and impact properties of this material. Also, other physical properties like low mass (ρ=1.25 g/cm^3) and its good behavior in humid environments present interest for their industrial use.

According to literature review, there is hardly any research with the purpose of developing the best functional models for studying the impact behavior of 3-D printed honeycomb cellular structures.

Thus, the present study emphases the research of next generation of honeycomb structures 3D printed from highly elastic, hard-wearing materials, in the aim of developing high energy absorption structures. The main focus of this work refers to the impact behavior of 3-D printed honeycomb structured materials via FDM, analyzing their capability of absorbing the impact energy, carrying out mechanical tests for material characterization. An effective energy absorbing structure will completely absorb the kinetic energy of a moving body whilst keeping the force on the body below a certain level. In order to analyze the energy absorption capability of the specimens, a comparative study of all the 4 test configurations has been performed. On this note, additive manufacturing process is explained from the CAD model to the final specimen. Afterwards, experimental results will be compared with FEM results.

2. Materials and methods

2.1. 3-D printing of cellular structures

A commercial polylactic acid (PLA) filament (Raise3D Premium PLA filament, 1.75 mm) with a density of 1240 kg/m^3 was used for the experiment. Young's modulus, tensile modulus, melting temperature, and elongation at break were 2636 MPa, 46.6 MPa, 150°C, and 1.9% respectively, as reported by the manufacturer [6]. During the printing process, the recommended nozzle temperature of the 3D printer for this PLA filament was set at 205°C. The printing parameters are presented in Table 1.

Table 1. 3-D printing parameters

Parameter		**Value**
Nozzle	Temperature (°C)	215
	Diameter (mm)	0.4
Infill	Density (%)	100
	Type	Rectilinear
Perimeters		2
Top/Bottom Layer		2
Heat bed temperature (°C)		60
Extrusion width (mm)		0.45
Layer height (mm)		0.2
Print speed (mm/s)		50
Volumetric flow (mm^3/s)		13
Extrusion width	Default extrusion width (mm)	0.45
	First layer (mm)	0.42
	Perimeters (mm)	0.45
	External perimeters (mm)	0.45
	Solid infill (mm)	0.45
	Top solid infill (mm)	0.4
	Support material (mm)	0.35
	Infill (mm)	0.45
Speed for print moves	Perimeters (mm/s)	60
	Small perimeters (mm/s)	15
	External perimeters (%)	50
	Infill (mm/s)	80

	Solid infill (mm/s)	20
	Top solid infill (mm/s)	15
	Support material (mm/s)	60
	Support material interface (%)	100
	Bridges (mm/s)	60
	Gap filling (mm/s)	20

The sandwich structures in this work were produced by Geeetech A30 3-D printing machine which uses FDM printing technology which consists in the extrusion of the polymer as it is induced into the machine in the form of a filament with a circular section, passing through a nozzle at ~~a~~ high temperature in order to shape the desired part (Figure 1). The final part is manufactured by the deposition of the melted material layer by layer. Among wide range of cellular structures, honeycomb pattern was selected in this study due to its high strength/weight ratio, the compressive strength of the honeycomb structures increasing with relative density.

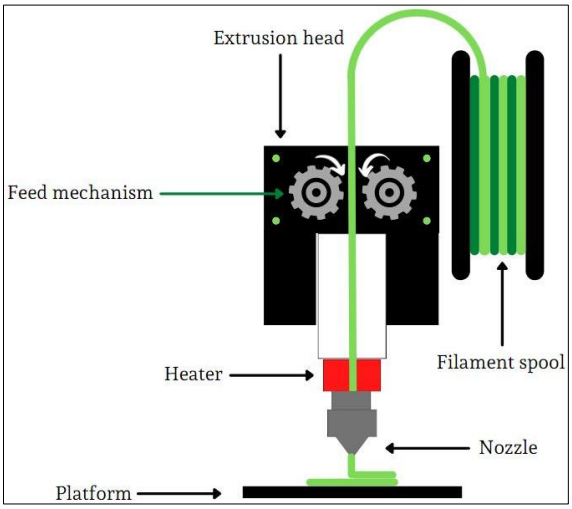

Figure 1. FDM process scheme

For impact tests, a special geometry according to this work has been chosen, namely a short-truncated cone (Figure 2), a geometry that has an analytical calculation model. Final piece also has the advantage of multiple modelling methods that can be adopted to make a finite element model.

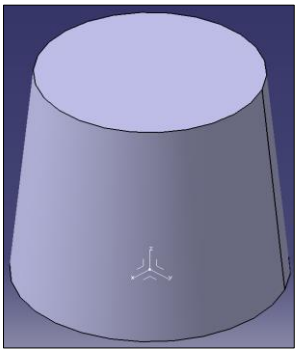

Figure 2. CAD design of the impact specimen (isometric view)

CATIA modelling is just one of the steps required in the manufacturing process. The next step is to generate the G Code for the numerically controlled production machine. This step is important because in the pre-processing software, all the printing parameters of the specimens are introduced: temperature, layer thickness, fiber orientation, etc.

2.2. Geometry aspects

Many researchers have conducted theoretical and numerical studies on conventional honeycomb structures under dynamic impact loading. The results have shown that for energy absorption the honeycomb structure is subjected to periodic plastic collapse deformation [7]. Some of the authors found that the mechanical properties of sandwich structures are strongly related to the properties of cell wall and its geometry [8]. Others have discovered that compressive strength of the honeycomb structure is independent of height and cell size but rather dependent upon their relative density [9]. As for printing process, compared to a solid FDM printed part, the build time of the honeycomb pattern increased about 65% because of its complex geometry.

By setting the parameters L_1, L_2 and θ, shown in Figure 3, to the values presented Table 2, the honeycomb geometry depicted in Figure 4b is obtained.

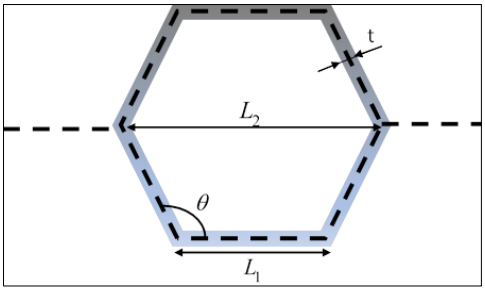

Figure 3. Layout of the hexagonal cell

Table 2. Geometric parameters of the employed hexagonal cell

	L_1 (mm)	L_2 (mm)	θ (°)	t (mm)
Honeycomb 1	4.12	8.25	60	0.45
Honeycomb 2	7.39	14.78	60	0.45

2.3. Finite element modelling aspects

Finite element modeling was performed on a 5% infill specimen. The initial condition is applied as an initial velocity in the nodes of the impactor mesh and has the value of -2.82 m/s (the negative sign shows that the orientation of the initial velocity vector is opposite to the orientation of the Z axis). In order to proceed into the finite element modelling, the geometry created in CATIA V5 has to be imported into the operating software (LS-Dyna) as a STEP file. This software is used as an analytical solver for analyzing the buffering characteristics of the honeycomb structures under dynamic impact loading.

After importing the geometry, design of the impactor along with its geometrical particularities was performed. Support plate was also created using the same software as for the impactor (LS-PREPOST).

After the numerical modelling of the impactor and support plate, discretization of the honeycomb structure was performed using two-dimensional triangular elements for all the surfaces.

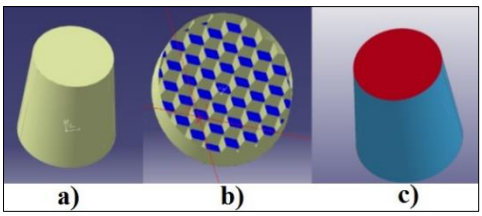

Figure 4. 3-D model in different software: **a)** CATIA surface model; **b)** CATIA model section view; **c)** LS-Dyna imported model

The geometry of the support plate consists in 100 mm width and 100 mm length. For its numerical modelling, quadrilateral elements were used (Figure 5). On each side there are 10 such elements with a

dimension of 10 mm wide and 10 mm long. The size of the items is large because this component is considered a rigid. So, the displacement and other mechanical stresses are not of interest, the plate having the role of preventing the translation of the honeycomb structure on the Z axis.

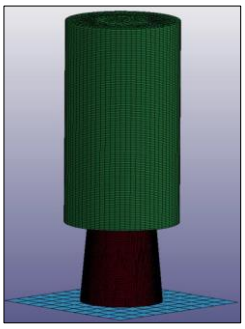

Figure 5. Components of the numerically modeled part; fixed rigid plate can be seen on the bottom side (blue), continuing with the honeycomb structured part and the impactor (green)

The modeled impactor, a cylinder with a diameter of 70 mm and a length of 125 mm, is equivalent to the real impactor. The mesh consists in three-dimensional hexahedral elements, also called as "brick". 70 elements are placed circumferentially and 125 elements in the impact direction.

After part discretization, material properties were defined. For support plate and impactor, a rigid material model was used. For preventing the instability, the properties of steel were used for both parts, in order to simplify the mass calculation. As for support plate's boundary conditions, the nodes are constrained in all directions. Also, the impactor translations on the X and Y axis are constrained. The boundary conditions, initial conditions and meshing details are summarized in Table 3.

Table 3. Numerical modelling setting

Part	Mesh elements	Material property	Boundary conditions	Initial conditions
Plate	2D quadrilateral element	Rigid	All degrees of freedom are constrained	-
Honeycomb	2D triangular element	MAT_059	Free	-
Impactor	3D hexahedral element	Rigid	Only Z-axis translation is allowed	Impact speed (2.82 m/s) applied in the opposite direction to the Z axis

2.4. Low velocity impact test

Low velocity impact tests were carried out on an Instron CEAST 9340 testing machine. This device offers a wide energy range (0.3 - 405 J), impact speed between 0.77 - 4.65 m/s and a drop weight between 1 - 37.5 kg. The test machine consists in two main components: the impact system and a data acquisition system. The equipment used in this investigation is provided with an experimental chamber for both high and cryogenic temperatures. The influence of temperature upon impact behavior of 3-D printed honeycomb structures is not discussed in this work. Therefore, all the impact tests were conducted at room temperature. The acquisition system was used for collecting data regarding the impact force and initial impact velocity of the sensor output. For this study, two types of honeycomb structures were designed: with 5% and 10% honeycomb infill (ratio between the part volume and the relative density). Two specimens were printed for each type, making a total of 4 pieces to be tested at different impact energies. All honeycomb specimens were manufactured with the same parameters (t=0.4 mm and θ=60°). Impact velocity was set to 2.82 m/s and the impact energy 15 J for one of the specimens with 5% honeycomb infill. In order to compare the influence of the infill percentage, two test probes with different infill were tested at 4 m/s impact speed and 30 J impact energy. The last specimen was tested at 4.62 m/s and 40 J.

3. Reesults and discussions

3.1. Experimental results

In the event of a low velocity impact, the disturbance is transferred from the point of impact in the form of longitudinal waves and transverse waves in outward direction. Thus, the energy is dissipated from the source (falling weight) to the impacted target (sandwich panel). The total energy during impact will be the sum of total energy absorption by the target, sound, heat and kinetic energy of flying particles. Further, the total energy absorption by the target is the sum of damage initiation and damage propagation. Energy-absorbing capacities of sandwich structures with honeycomb under impact are closely linked to the core crushing. Core crushing is a complex mechanical phenomenon characterized by the appearance of various folds and failures in the hexagonal structure.

The impact response of developed PLA honeycomb structures at impact energies of 5, 30 and 40 J is presented as force-time (f -t) histories in Figure 6.

The PLA 10% honeycomb tested specimens presents for both 30 and 40 J energies a similar behavior characterized by a linearly and quickly increasing trend of the force as the impact develops, due to the elastic modulus of the structure. Then the force reaches a stable and fluctuant state. A stable phase is mainly due to the buckling property of the honeycomb core in the experiment, where the top facesheet damage cause the fluctuations. The progressive damage is described by the oscillation in the curve from the loading and unloading of the impactor. The trend continues up to a maximum value, usually identified as Peak Load (around 2.5 kN for both 10% infill honeycomb tested). At last, the contact force decreases gradually with the impactor rebounding. Nevertheless, although both PLA 10% infill honeycomb tested specimens presents similar stiffness for both 30 and 40 J impact energies, it is clear that at 40 J the decrease in contact force is delayed and the deformation is higher indicating higher energy absorption.

For the 5% infill PLA honeycomb tested specimen for 30 J (blue curve Figure 6), the impact response has a similar trend and a comparable maximum peak load as the 10% infill PLA honeycomb tested specimen at same energy (green curve Figure 6). Nevertheless, the load increasing trend up to the maximum value of Peak Load starts around 10 ms elapsed time, corresponding to 20 mm displacement. The very first peak load, appears shortly after the impact and is 2.5 times lower. Likewise, the deformation is nearly 2 times higher (around 45 mm) indicating significantly higher energy absorption.

For the 5% infill PLA honeycomb tested specimen for 15 J (red curve Figure 6), an unusual behavior is exhibited. The very first peak load is similar to the one obtained on the 5% infill PLA honeycomb tested specimen for 30 J (blue curve Figure 6), followed by a decreasing oscillation domain and a second first peak load comparable with the first one (at 770 N), then a decrease in load. The 35 mm displacement measured is lower than the one obtained on the 5% infill PLA honeycomb tested specimen for 30 J, indicating a lower energy absorption. This impact response is very similar to the NOMEX honeycomb structures [8, 9]. The multi-varied damage mode is specific to the yielding of a brittle material. The increase of the average value of the force in the first 0.57 milliseconds and up to the absolute maximum is given by the confining of the material inside the honeycomb. This phenomenon is due to the damage mode characterized by the gradual failure of the structure inside.

No smooth course was observed and all tested specimens exhibits oscillations on the force-time curves, suggesting progressive damage by local failures in the specimen due to the decrease in the structural stiffness (near the impact point).

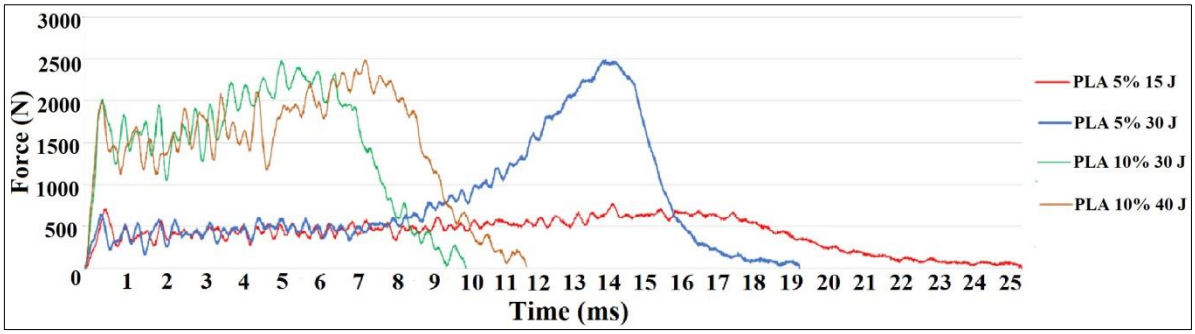

Figure 6. The dynamic response of all test specimens

Figure 7 illustrates the results obtained for the low velocity impact tests on all honeycomb structures subjected to several incident kinetic energies.

Figure 7 shows that the dependence between energy and displacement (which represents the structural deformations in the direction of the Z axis) is almost linear. In the last moments of the impact when the deformations reach high values and the impacted material collapsed inside the structure, the energy is suddenly transferred to a solid material consisted of the previous yielded material. The impact energy was 15 J for the 5% infill specimen but a value of 16.06 J is recorded in the graph. The energy difference is given by the potential energy of the falling impactor, transformed into kinetic energy on the distance in which the impactor deforms.

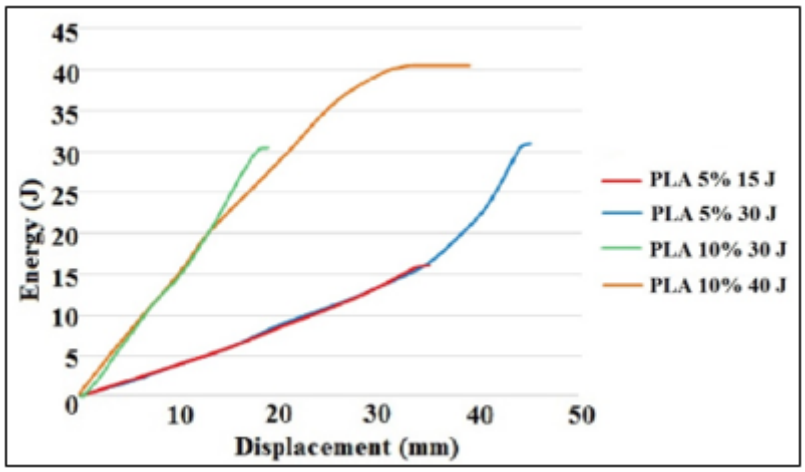

Figure 7. Energy (J) - displacement (mm) curves of the tested structures

The initial impact speed was 2.82 m/s for the 5% infill specimen at the initial moment of impact. As expected, the deformation of the samples increases with impact velocity. Figure 8 shows that the velocity variation is almost linear during the impact, but less in the densification stage due to the collapse of the material.

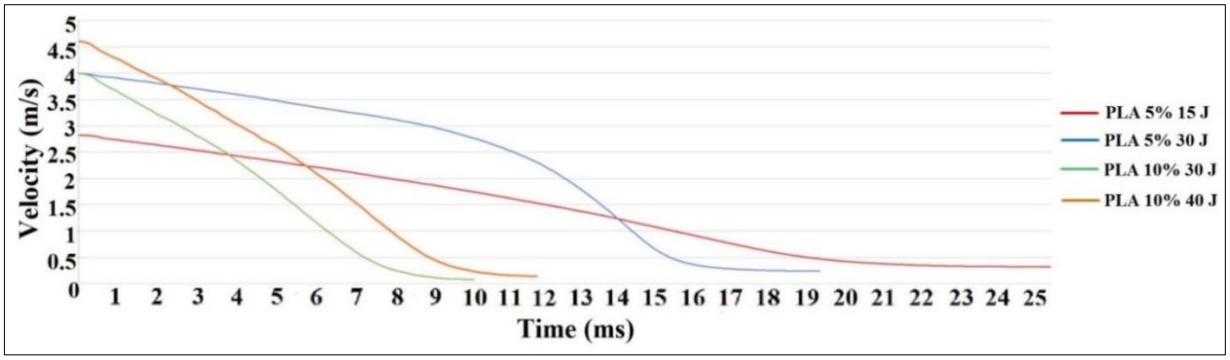

Figure 8. The velocity time-history curves of the tested structures

Figure 8 illustrates the velocity response of the impactor head during 30 J dynamic test (specimen PLA 5% 30 J). One observes from the results in such a figure that the higher impact loading (30 J) produces higher rebound velocities than the lower impact loading (15 J). Also, the velocity varies linearly until absolute maximum is reached.

Figure 9a shows images of the 5% honeycomb specimen (PLA 5% 15 J), impacted at different timeframes, from the initial moment (t=0 ms) of impact. It is observed that the specimen has a 5-degree angle to the side walls. However, Figure 9b represents the deformation of the structure when the force resulting from the impact reach the highest point, it can be noticed that the structure gives way by collapsing inside itself. A comparison of the damage mode between FEM and experiment will be presented in the next section. It was expected that the yielding of the part to be at the top, in the minimum section size, but it yielded when it reached its middle section. This may be due to defects in the structure such as: strong variations in the flow of extrusion leading to the lack of material in the yield zone, the condition of the raw material before the printing process could have been altered humidity or UV exposure of the polymer, the existence of some inclusions such as dust or air gaps etc. The maximum damage can be seen in Figure 9c.

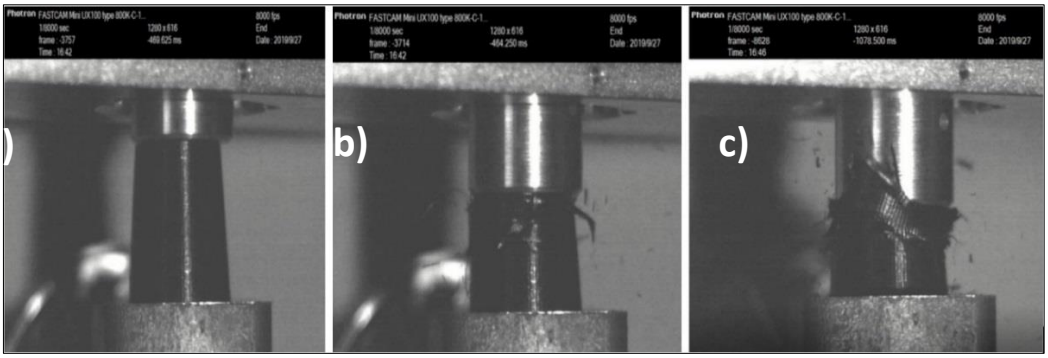

Figure 9. 5% honeycomb specimen, impacted at different timeframes:
a) t=0 ms, **b)** t=1.3 ms, **c)** t=24 ms; 15 J impact loading

The third set of tests is performed on 10% honeycomb specimens at a 30 J impact loading and a velocity of 4 m/s. It can be seen in Figure 6 that as the honeycomb content increases, so does the maximum force, by 3.24 times compared to 5% honeycomb specimens impacted at the same velocity. The absolute maximum is not located at the beginning of the impact; it's recorded to be at the end of the impact. The confined material hypothesis might explain the emergence of such a late maximum. As shown in Figure 7, the variation of the energy deformation is proportional to the displacement. As the energy increases, so does the displacement. It is clearly that with the increase of the honeycomb content, the amount of absorbed energy grows higher, but so does the forces during the impact. The velocity varies almost linearly and even more pronounced than in the other test pieces so far. So, compare to the 5% honeycomb specimens and from analyzing the results given, it is clearly that with the increase in honeycomb content, it results in a more sudden failure of the sample.

The last test configuration has 10% honeycomb infill with a 30 J impact loading and a velocity of 4.6 m/s. The mass of the assembly that forms the impactor is 3.76 kg. Compared to other high-density honeycomb specimens, the increase in impact loading does not lead to an increase in the contact force between the impactor and the test-piece, as in the case of metals. The visual observations of the deformation patterns exhibited by the examined specimens under low velocity impact tests highlighted the occurrence of the highest strain concentrations in the proximity of the indentation head, similar failure mechanisms can be seen for all types of structures, regardless of the impact loading value.

Several frames extracted from the recordings obtained of the 10% honeycomb content specimen can be seen in Figure 10. Same damage mode can be observed as in the case of the other specimens. Analysis of these results reveals that all loading conditions produce noticeable damage of all the examined structures.

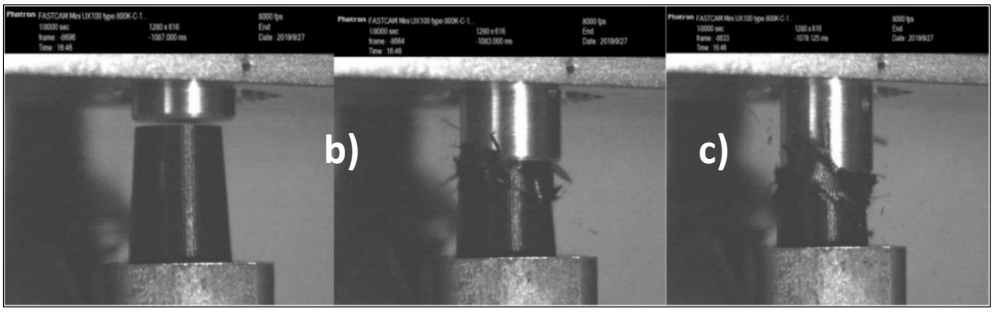

Figure 10. 10% honeycomb specimen, impacted at different timeframes: a) t=0 ms, b) t=1.3 ms, c) maximum displacement; 40 J impact loading

3.2. Comparison between experimental results and FEM results

The results obtained from the FEM analysis were compared with the experimental data. Figure 11 shows the experimental test and the finite element model before and after the impact. The geometric differences of the impactor are justified by the need for a larger volume of material to compensate for the mass of the device on which the impactor was actually mounted.

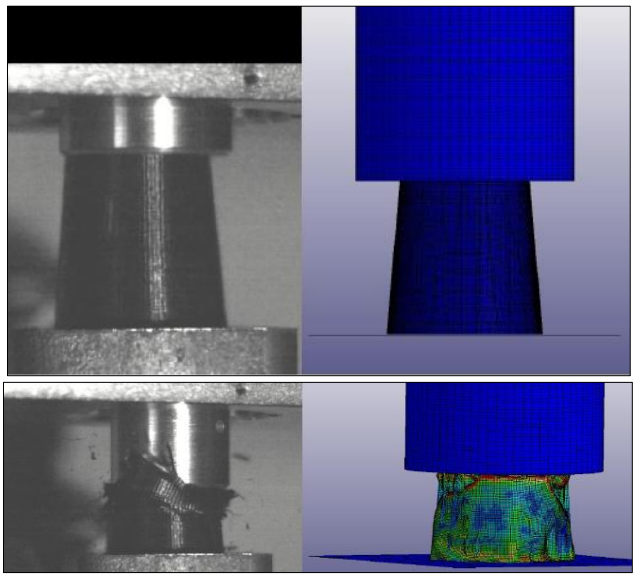

Figure 11. Comparison of the maximum displacements between the finite element model and the real model before and after the impact (PLA 5% 15J)

Figure 11 shows the deformation of the real structure and the idealized structure. It can be seen that in terms of quality, the deformity obtained from finite element modeling is similar to the real one, with small differences in the yield of the test specimen walls. At a quantitative level, the idealized structure has maximum displacements of only 25 mm, compared to the real structure which has deformations of 35 mm. The differences between the two structures may be due to errors in the specimens' manufacturing process, such as variations in the diameter of the filament leading to insufficient or abundant extrusion of material locally.

In Figure 12 the idealized structure is more rigid than the real one by the fact that the forces resulting from the contact are very large. The first peak of the force of about 1200 N may be due to the mathematical modeling of the contacts. The results of the numerical model provide a visible region between the first and second peak loads, which is governed by core damage. In the experiment, this region is not evident to notice because the failed elements are not deleted and this leads to densification, as already reported in previous studies [11]. Figure 13 presents the displacement recorded over time for

both numerically and experimentally analysis, showing a higher displacement value in the experimental case, potentially due to both boundary definition and the mathematical modeling of the contacts. Nevertheless, the discrepancies between the numerical and experimental results are acceptable to assess the overall performance from an engineering perspective.

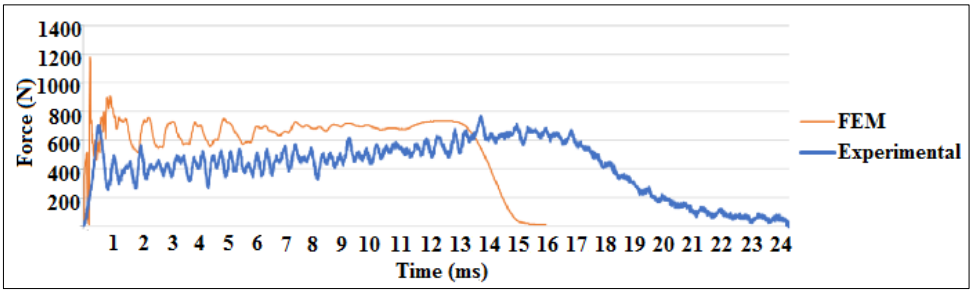

Figure 12. The dynamic response of the structure obtained with the finite element method and by processing the experimental data (PLA 5% 15J)

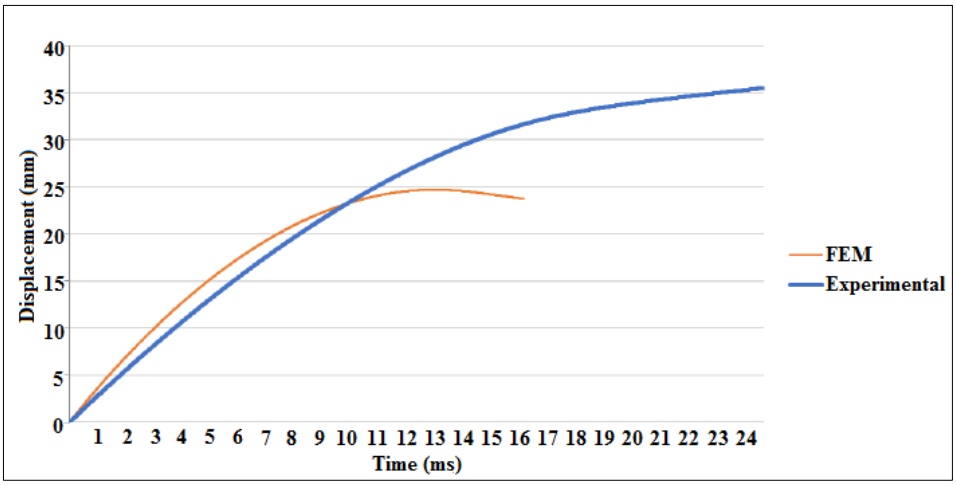

Figure 13. Comparison of displacements in the finite element model and experimental results (PLA 5% 15J)

The history of energy as a function of time curves during impact for the modeled case and its experimental equivalent are shown in Figure 14. The absorbed energy of the honeycomb specimens increases with increasing impact energy and then shows a slight decline until it reaches a constant value of energy with the increase of impact time. It can be seen that for the finite element model the energy absorption is faster compared to the energy variation for a real test specimen.

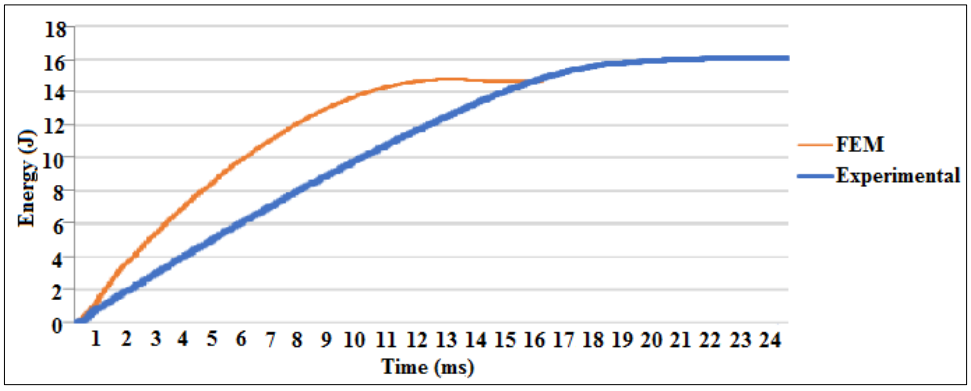

Figure 14. The energy absorbed during the impact (PLA 5% 15J)

There are also similarities between the two curves, both being characterized by an almost linear portion of energy absorption. Compared to the experimental case, there is an amount of energy absorbed by the idealized structure with finite element because in reality the impactor also gains energy from the conversion of potential energy into kinetic energy during the deformation of the specimen. In the analysis of an impact, the most important quantity is the energy consumed for the deformation of the structure, and the quantities such as maximum displacements or stresses are not of major interest.

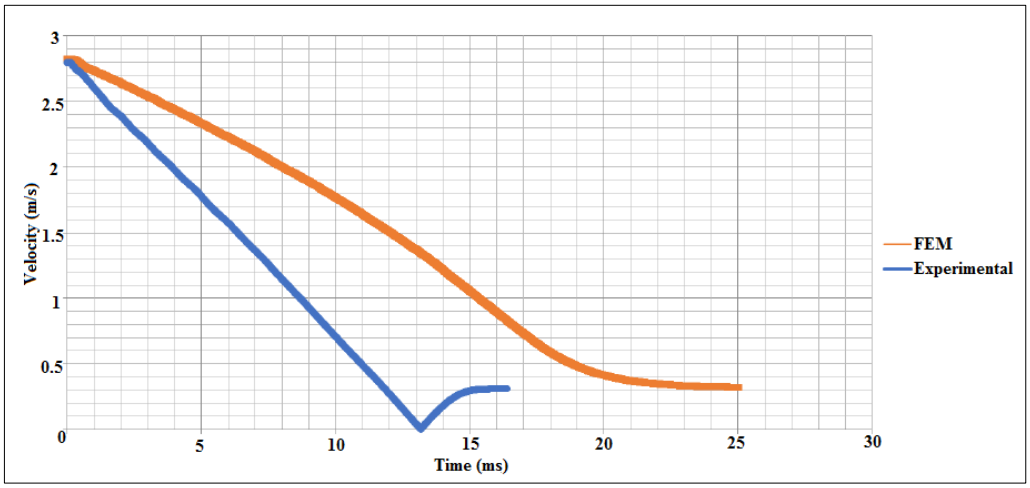

Figure 15. Velocity variation in the finite element model and experimental results (PLA 5% 15J)

Figure 15 shows the variation of the impactor speed over time. The velocity varies almost linearly in both cases. It is observed that the variation is more sudden for the modeled structure and that when the speed reaches the value of zero there is a transfer of energy from the structure back to the impactor. That energy given to the impactor represents the energy absorbed, but not dissipated by the honeycomb structure. It should be noted that the recoil speed of the impactor is equal in both cases. The main difference between the finite element model and the experimental values is that the speed variation is much more sudden.

Figure 16 shows the buckling of honeycomb cells in the finite element model showing similar failure morphology as sample after the experimental tests. It is noteworthy that the deformity is similar to that of metal honeycombs as presented in [10] or composite hexagonal honeycombs [13]. The dent depth, force response, and deformation mechanism of the remaining samples were in agreement with the experimental results. The impact damage was localized at the impacted zone, the failures were dominated by the fracture of face sheets, crushing, buckling and breaking of the cell walls of the honeycomb cores.

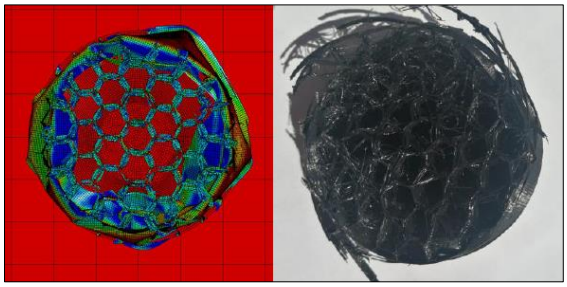

Figure 16. Honeycomb buckling (comparison between finite element modeling and tested specimen)

4. Conclusions

By 3D printer technology, honeycomb structures can be produced in desired geometries, and tailored properties with improved impact strength and energy dissipation ability. The 3D printed using FDM technology PLA 5 and 10% honeycomb infill impact specimens have proven useful as energy absorption structures. Experimental results showed that both PLA 10% infill honeycomb specimens (tested at 30 J and 40 J) exhibits higher stiffness compared with PLA 5% infill honeycomb specimens. Nevertheless, for the same impact energy (30 J) one of the PLA 5% infill honeycomb specimen displayed similar impact resistance as PLA 10% infill honeycomb specimen and significantly larger deformation. Although similar stiffness was observed on both PLA 10% infill honeycomb specimens, for the one tested at higher impact energy (40 J) the deformation was nearly two times higher. The 35 mm displacement measured for 5% infill PLA honeycomb (15 J) is lower than the one obtained on the 5% infill PLA honeycomb 30 J tested specimen, indicating a lower energy absorption, nevertheless although it presents also low stiffness compared to the others 3D printed PLA tested specimens, the impact response is very similar to the NOMEX honeycomb structures. Furthermore, a finite element model was developed for one of the impact cases in which the development of a model that could predict the amount of energy absorbed by the structure was sought. The entire finite element modeling was performed in the LS-Dyna software. Likewise, the amount of energy absorbed during the impact, the failure and degradation of the impacted specimens were monitored, following the analysis of experimental and numerical data. It can be concluded that 3D printed honeycomb using FDM technology PLA 5% and 10% honeycomb infill impact structures have acceptable energy absorption capacity under low velocity impact, comparable to that of metallic [14], hybrid [8] and composite [11, 13] materials honeycomb structures.

References

1.CANTWELL, W.J., MORTON J., Comparison of the low and high velocity impact response of CFRP, *Composites*, **20** (6), 1989, 545-551
2.SCHAEDLER, T.A., CARTER, W.B., Architected cellular materials, *Annu Rev Mater Res*, **46**, 2016, 187-210
3.GIBSON, L.J., ASHBY, M.F., *Cellular solids: structure and properties*, Publisher: Cambridge University Press, New York, 1999
4.ALLEN, H.G., *Analysis and design of structural sandwich panels: the commonwealth and international library: structures and solid body mechanics division*, Publisher: Pergamon, 2013
5.JARDINI, A., FILHO, R. M., SAVIOLI LOPES, M., Poly (Lactic Acid) Production for Tissue Engineering Applications, *Procedia Engineering*, **42**, 2012, 1402-1413.
6.DRUMRIGHT, R., GRUBER, P., HENTON, D., Polylactic Acid Technology, *Adv. Mater.*, **12**, 2000, pp. 1841-1846.
7.CORAPIA, D., MORETTINIA, G., PASCOLETTIA, G., ZITELLIA, C., *Procedia Structural Integrity AIAS 2019 International Conference on Stress Analysis*, 24 (2019) pp.289-295.
8.XIE, S., JING, K., ZHOU, H., LIU, X., Mechanical properties of Nomex honeycomb sandwich panels under dynamic impact, *Composite Structures*, **235**, 2020, 111814
9.RUPP, P., IMHOFF, J., WEIDENMANN K. A., Low-Velocity Impact Properties of Sandwich Structures with Aluminum Foam Cores and CFRP Face Sheets, *J. Compos. Sci.*, 24, 2(2), 2018
10.CHAWLA, A., MUKHERJEE, S., KUMAR, D., NAKATANI, T., UENO, M., Prediction of Crushing Behavior of Honeycomb structures, *International Journal of Crashworthiness*, **8 (**3), 2003, 229-235
11.USTAA, F., TÜRKMENA, H. S., SCARPA F., Low-velocity impact resistance of composite sandwich panels with various types of auxetic and non-auxetic core structures, *Thin-Walled Structures*, **163**, 2021, 107738
12.TIJU, T., TIWARI, G., Crushing Behaviour of Honeycomb structure: A Review, *International Journal of Crashworthiness*, **24 (**5), 2019

13.ÖZENA, İ., ÇAVAB K., GEDIKLIA, H., ALVERB, Ü., ASLANB, M., Low-energy impact response of composite sandwich panels with thermoplastic honeycomb and reentrant cores, *Thin-Walled Structures*, **156**, 2020, 106989
14.FOO, C.C., SEAH, L.K., CHAI, G.B., Low-velocity impact failure of aluminium honeycomb sandwich panels, *Composite Structures* **85**, 2008, pp. 20-28.

Manuscript received: 2.03.2022